VNU Journal of Science: Natural Sciences and Technology, Vol. 40, No. 3 (2024) 82-89

VNU Journal of Science: Natural Sciences and Technology

Journal homepage: https://js.vnu.edu.vn/NST

Original Article

$ZnCo_2O_4$ and the Role of K_2CO_3 for Highly Advanced Oxidation over Methylene Blue Degradation

Do Huy Hoang, Trieu Thi Nguyet*

VNU University of Science, 19 Le Thanh Tong, Hoan Kiem, Hanoi, Vietnam

Received 07th May 2024
Revised 16th May 2024; Accepted 31st May 2024

Abstract: $ZnCo_2O_4$ spinel nanomaterial modified in the glass phase of K_2CO_3 demonstrated the highly advanced oxidation in the mild condition of no light and low temperatures (5 ^oC) to degrade the pollutant model of methylene blue up to the yield of ~95% (25 ^oC) and ~ 51% (5 ^oC) with a molar ratio of Zn:Co:K = 1:2:1. As-products from degrading the solution of methylene blue expressed no signal for the Uv zone in Uv-vis absorption spectra as the signature for aromatic bones which is the superiority of the material for converting methylene blue to non-aromatic compounds, even to CO_2. $ZnCo_2O_4$ was prepared through the co-precipitation of bi-metallic hydroxide and then calcination with the presence of K_2CO_3. By XRD, EDX, SEM, and BET, it was confirmed that the product contains only one phase of cubic spinel nanocrystals with a relatively large size and a small surface area, in which the molar ratio of metals in the product is almost the same with the initial mixture.

Keywords: $ZnCo_2O_4$ /K_2CO_3, methylene blue, highly advanced oxidation, without light.

1. Introduction

The materials with a spinel structure have gotten some attention for their resistance to oxidizing/reducing agents and their application in many fields such as pigments, refractory, electronic engineering, magnetism, and energy storage materials. Spinel structures with Zn element may be a good photo-catalytic direction such as $ZnFe_2O_4$, $ZnCr_2O_4$, $ZnCo_2O_4$,... [1] with a belief on photocatalytic enhance through ion Zn^{2+} for the pollution treatment under visible light. However, the requirements of light exposure for photo-degradation over solid catalysts, in general, can sometimes be a drawback for industrial application of water treatment due to the limitation of sun shining time or the energy to produce the UV or visible light.

The combination of Zinc with multiple-oxidation-state elements from group VIIb in the periodic table of elements may be an advanced choice through the Fenton-like reactions. $ZnCo_2O_4$ is synthesized by various methods, such as hydrothermal [2-4], co-precipitation [5, 6], and co-precipitation combined with doping of other metal ions [7-10]. The application possibilities of ZCO material are

---

[*] Corresponding author.
E-mail address: nguyetdhkhtn@gmail.com

https://doi.org/10.25073/2588-1140/vnunst.5674

abundant, such as for energy storage [11, 12], ciprofloxacin treatment in the presence of persulfate under microwave conditions [3], and photocatalytic ability to treat dyes like methylene blue (MB) in aqueous solution under normal light conditions [4, 5, 13, 14]. The published reports on the photocatalytic ability of nano spinel $ZnCo_2O_4$ showed that this material adsorbs a small amount of pollutants in the dark. The catalytic ability of the material is quite strong in both visible and UV light, which is entirely consistent with the small band gap energy value (~2.1 eV) of $ZnCo_2O_4$ [1]. Doped $ZnCo_2O_4$ materials were mentioned to introduce metal ions with sizes similar to Zn^{2+} or Co^{3+} into the crystal lattice.

Table 1. The various preparations and applications of $ZnCo_2O_4$

No	Preparation	Application/yield	Ref.
1	Hydrothermal	MB photodegradation/sunlight with ultrasound, 180 min, 91%	[1]
2	Hydrothermal coprecipitation/modified with ZrO_2	2-chlorophenol, adsorption of 14% in the dark, photodegradation/ visible light, 91%	[4]
3	Co-precipitation	MB photodegradation/visible light,	[5]
4	Co-precipitation/modified with MnO_2/FeS_2	Methyl orange photodegradation/visible light, 80 min/ 96%	[7]
5	Co-precipitation/modified with $CaFe_2O_4$	Tetracycline photodegradation/visible light, 100 min, 88%	[8]
6	Co-precipitation/modified with Ag@AgCl	rhodamine B (RhB) photodegradation/visible light, 120 min, 99%	[9]
7	Sacrificial template accelerated (STAH) method	MB photodegradation/visible light, 210 min, 96%	[13]
9	Co-precipitation modifying with K_2CO_3	MB degradation, no light, 60 min, ~94%	This work

This strategic improvement of the material's properties through modifying the surface is a key focus of our research, as it can enhance the performance of $ZnCo_2O_4$ in various applications. In this work, we address the influence of using K_2CO_3 in the synthesis process to promote the catalytic ability of $ZnCo_2O_4$ nanomaterials with two purposes. Firstly, using the melting alkaline K_2CO_3 (melting point at 891 °C) is to improve the solid reaction between ZnO and CoO in the air. Secondly, the glassy state of K_2CO_3 after cooling down might respond to separating the small crystal of $ZnCo_2O_4$ as a solid surfactant. The photocatalytic results interestingly had no superiority to the highly advanced oxidation under no light conditions, at cold temperatures (5 °C), which is the novelty of our research.

2. Experiment

$Zn(NO_3)_2 \cdot 6H_2O$ (Sigma-Aldrich, 99%), $Co(NO_3)_2 \cdot 6H_2O$ (Sigma-Aldrich, 98%), KOH (Sigma-Aldrich, 85%), K_2CO_3 (Korea, 99%.), Methylene Blue hydrate $C_{16}H_{18}ClN_3S \cdot xH_2O$ (Sigma-Aldrich, 97%).

2.1. Material Preparation

Take an amount of $Zn(NO_3)_2 \cdot 6H_2O$ and $Co(NO_3)_2 \cdot 6H_2O$ in a molar ratio of 1:2, transfer it to a glass cup, and add distilled water to dissolve the crystals. Slowly add the resulting solution into another glass cup containing hot water, and stir until the solution boils gently for about 5 minutes. Let the solution cool to room temperature, then slowly add enough 5% KOH solution to precipitate the hydroxide of the metal ions into the beaker. Continue stirring the reaction mixture for about 30 minutes. Filter the precipitate on an air suction filter and wash it several times with distilled water until the washing water has pH=7. Dry the precipitate at room temperature in a vacuum oven.

Take a quantity of K_2CO_3 crystals mixed with the solid obtained above and grind with a mortar and pestle, then ignite at 1000 ^oC for 4 hours. Allow the solid to cool gradually in the furnace to room temperature. Grind the product to obtain ZCO material.

The structure and crystalline composition of the material were studied by powder X-ray diffraction (XRD) on a D8 X-ray diffraction device (Burcker, Germany) using CuKα radiation (λ = 1.54056 Å) at the Department of Inorganic Chemistry, Faculty of Chemistry, University of Natural Sciences.

The morphology and grain size of the material samples were studied based on scanning electron microscope (SEM) images on a Nova NanoSEM 450 (FEI, Netherlands) at the Center for Materials Science, Department of Physics, University of Science.

The material's element component was determined based on the energy dispersive X-ray spectroscopy (EDX) method on the TEAM Apollo XL EDS machine (EdAx, USA) at the Center for Materials Science, Department of Physics, University of Science.

The surface area of the material was studied using a nitrogen isothermal adsorption-desorption (BET) on Tristar II 3020 3.02, (Micromeritics, USA), Institute for Tropical Technology.

2.2. Decomposition of Methylene Blue

Add 100 mg of material into 100 mL of MB solution with a concentration of 10 ppm and stir on a magnetic stirrer. After each specified period, the amount of solution used to determine the MB concentration is taken. The MB concentration in the solution was determined by measuring optical absorbance on an ultraviolet-visible molecular absorption spectrometer V-630 (Jasco, Japan). Deuterium lamps and halogen lamps were the light sources used with a silicon photodiode detector and a 1 cm thick quartz cuvette. MB decomposition yield (H%) was calculated according to the following formula:

$$H = \frac{C_o\text{-}C_t}{C_o} \times 100$$

C_0 and C_t are the concentration (mg.L^{-1}) of MB in the solution at the initial time and time t, respectively. The determination was performed at the Department of Inorganic Chemistry, Faculty of Chemistry, University of Sciences.

3. Result and Discussion

3.1. Materials Preparation

In the first step of materials synthesis, a mixed solution of Zn^{2+} and Co^{2+} salts with a molar ratio corresponding to the composition of spinel $ZnCo_2O_4$ was added to hot water so that the hydrolysis of cations occurred faster, then slowly add KOH solution to precipitate the metal hydroxides. The amount of KOH needed is just enough to avoid dissolving zinc hydroxide. This stage dramatically affects the crystal size [1]. The calcination process occurred at high temperatures in air, so Co^{2+} was oxidized to Co^{3+}. Adding K_2CO_3 into the solid before calcination increased the possibility of creating a spinel phase because K_2CO_3 was considered a liquid alkaline. In Figure 1, peaks of the X-ray diffraction at (220); (311); (222); (400); (422); (511); and (440) are in perfect agreement with the cubic structure of spinel $ZnCo_2O_4$ according to the data of JCPDS No 23-1390 [1].

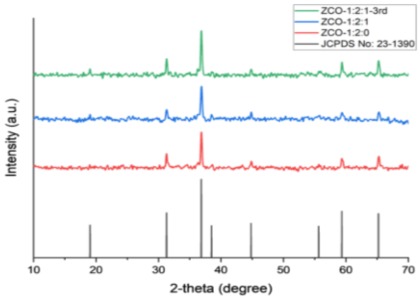

Figure 1. X-ray diffraction pattern of $ZnCo_2O_4$ with different starting molar ratios of Zn:Co:K and the 3rd recycled one.

The diffraction pattern showed that the obtained material had only one crystalline phase, $ZnCo_2O_4$, with a cubic structure and a crystal size of ~40 nm. Changing the amount of K_2CO_3 during synthesis has little effect on the lattice constant and crystal size (Table 2). K^+ may not enter the spinel lattice because the size of this cation is much larger than that of the metal cations Zn^{2+} and Co^{3+}.

SEM image (Figure 2) shows that the particle size is relatively large and uneven due to the accumulation of $ZnCo_2O_4$ crystals. The EDX spectrum of ZCO_1 (Figure 2) shows that the elements Zn, Co, and K are present in the material's composition, with the molar ratio Zn:Co:K = 1:1.7:1, almost similar to the molar ratio of the starting substances.

Table 2. Lattice constants and crystalline size of ZCO

No.	Sample	Initial molar ratio Zn:Co:K	2θ	FWHM	a=b=c (Å)	r (nm)
1	ZCO_0	1:2:0	36.856	0.190	8.081	44.0
2	$ZCO_{0.2}$	1:2:0.2	36.828	0.204	8.086	41.1
3	$ZCO_{0.4}$	1:2:0.4	36.850	0.204	8.059	41.0
4	ZCO_1	1:2:1	36.875	0.243	8.040	34.5

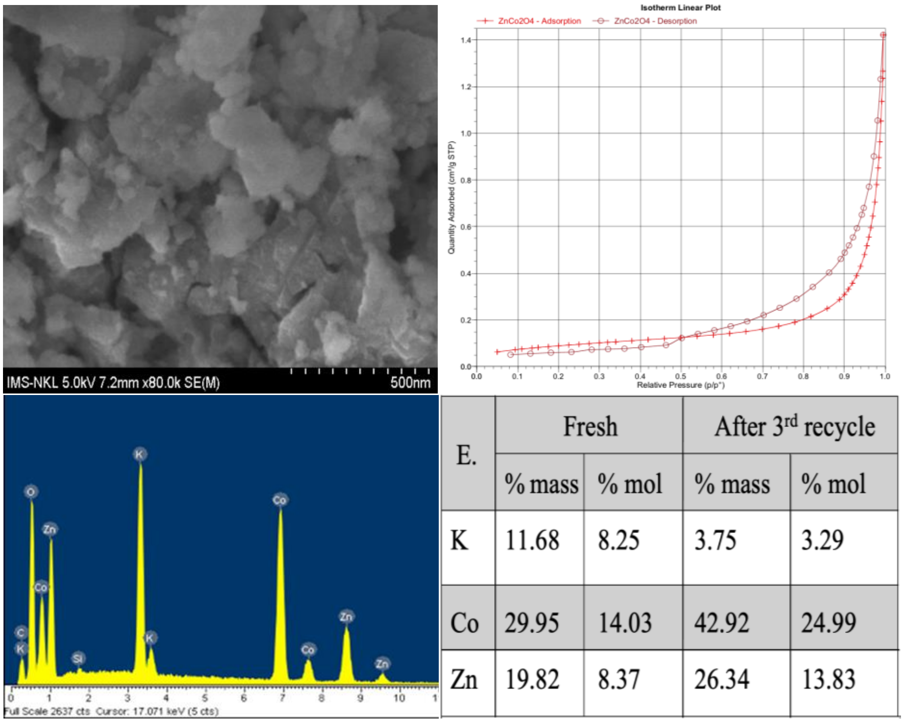

E.	Fresh		After 3rd recycle	
	% mass	% mol	% mass	% mol
K	11.68	8.25	3.75	3.29
Co	29.95	14.03	42.92	24.99
Zn	19.82	8.37	26.34	13.83

Figure 2. SEM, BET, and EDX spectrum of ZCO_1.

At a heating temperature of 1000 °C, K_2CO_3 melts to form a glassy state where $ZnCo_2O_4$ crystals are dispersed in a glass phase to form the more complicated structure of material. The EDX expresses the larger ratio of carbon to potassium which may be explained by the absorption of CO_2 from the air or the intrusion of K^+ into $ZnCo_2O_4$ crystals.

The surface area of the material determined by BET is relatively small, equal to 0.325 m^2/g. The above data shows that the synthesized material is $ZnCo_2O_4$ nano spinel dispersed in amorphous K_2CO_3 with large particle size and small surface area.

3.2. Methylene Blue Degradation

The UV-Vis spectra of MB solution after different periods exposing ZCO_0 without K_2CO_3 and ZCO_1 with K_2CO_3 are given in Figure 3 and Table 3.

The results showed that ZCO_0 without K_2CO_3 has weak MB adsorption and photocatalytic decomposition of MB under normal light conditions, as the same data with the reference [8] showed. Excitingly, the ZCO_1 without K_2CO_3 decolorizes MB with a very high yield, regardless of the light source, and with a fast decoloration rate.

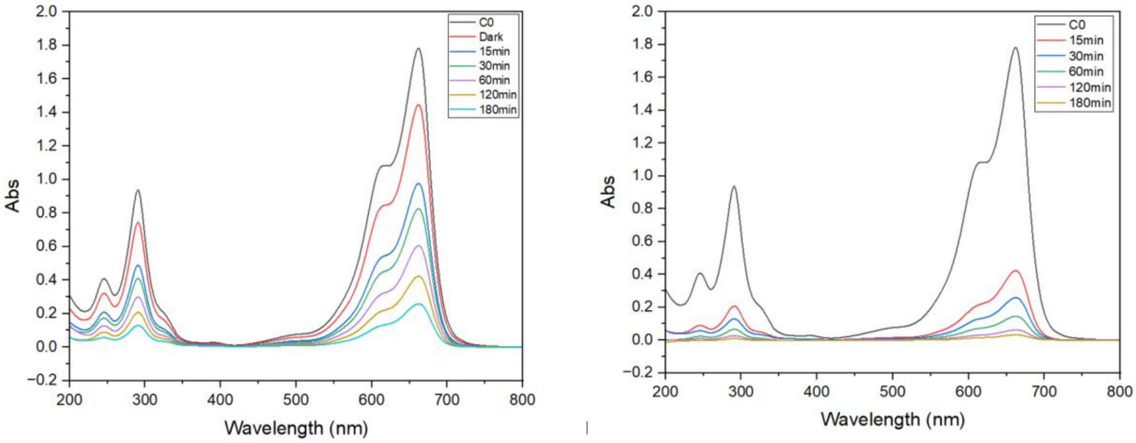

Figure 3. The UV-Vis spectrum of MB solution over time in the presence of ZCO_0 without K_2CO_3 in darkness and normal light (left) and ZCO_1 with K_2CO_3 in darkness (right).

Table 3. Decoloration of MB over time in the presence of ZCO material

ZCO_0 without K^+			ZCO_1 with K^+		
Light condition	Time (min)	Yield (%)	Light condition	Time (min)	Yield (%)
Dark	30	11.3	Dark	15	80.6
Normal light	15	45.1		30	87.2
	30	53.6		60	93.8
	60	64.9		120	96.1
	120	76.2		180	97.3
	180	85.5	With light (normal light, UV, infrared)	120	95-97

The UV-vis spectrum in Figure 3 of the MB solution after the catalytic process with ZCO material shows a significant reduction of all adsorption peaks at 664 nm, 613 nm in the visible region, and 246 nm, 292 nm in the UV region. The adsorption peaks in the visible region corresponding to the n-π* transition of the MB molecule. In contrast, the adsorption peaks in the ultraviolet region correspond to the π -π* electron transition. The decrease in the signal of MB on the UV-vis spectrum in both the ultraviolet and visible demonstrates the radical breaking of bonds on the MB molecule to form secondary products without π bonds or characteristic aromatic ring, which can then produce CO_2.

The ability of ZCO material to degrade MB over time is shown in detail in Table 3. Obviously, with the bare ZCO_0 catalyst not modified with K_2CO_3, the photo-oxidation decomposition rate of MB occurs relatively stable and reaches 85% efficiency after 3 hours under visible. Meanwhile, the ZCO_1 catalyst in the presence of K_2CO_3 shows an outstanding ability to treat MB with high reaction speed, reaching 80.6% after only 15 minutes of the experiment. Still, after that, the MB degradation speed slows down and reaches 97.3% after the next 180 minutes. On the other hand, MB decomposition experiments in the presence of ZCO_1/K_2CO_3 under different light conditions, such as normal, infrared, and UV light, did not significantly improve MB treatment efficiency, reaching 95-97%. The ZCO_1/K_2CO_3 material, thus, can catalyze high-performance redox reactions, similar to the Fenton reaction in no need of light. To facilitate further research, we chose normal artificial light conditions under wall compact lamps in the laboratory to perform.

Figure 4 shows the effect of temperature on the MB decoloration yield of ZCO_1 material after 60 minutes under normal light conditions. MB degradation yields increased significantly when the temperature was increased from 5 °C to 25 °C and then decrease slowly when the temperature continued to rise to 50 °C. The above results allow us to predict that the discoloration of MB in the presence of ZCO_1 material is not wholly due to physical adsorption but may be due to chemical adsorption or the material's catalytic role. At experimental conditions at 50 °C, the efficiency of the degradation decreases by an insignificant 10% (92% at 25 °C and 82% at 50 °C). Physical adsorption processes often tend to decrease efficiency as temperature increases, which may be consistent with experimental results but not be the main factor. It is proposed that the higher temperature may decrease the ability of MB reaching to the surface of ZCO which makes the degradation processes slower.

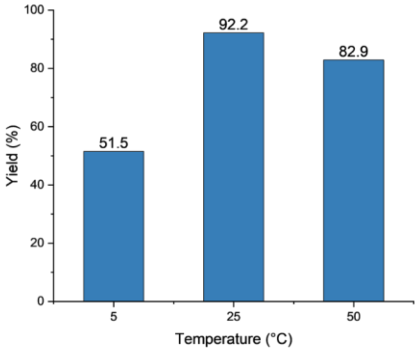

Figure 4. MB decoloration over ZCO_1 at different temperatures in normal light.

To confirm the role of highly advanced oxidative ZCO1, the recycle experiments were performed (Table 4). The catalyst, after each time used, was cleaned gently with water and then dried naturally in the air. The degradation of MB over ZCO_1 remains relatively high after three reuses.

Our comprehensive analysis with XRD (Figure 1) and EDX (Figure 2) has unequivocally demonstrated that the crystal structure exhibits remarkable stability, remaining unchanged after three reuses but the chemical composition of the material has minor changes in the K content. This steadfastness, with the molar ratio of Zn:Co = 1:1.8 remaining almost identical to the original ZCO_1, inspires confidence in the material's integrity. Notably, the K content did decrease significantly, a change possibly attributed to the dissolution of the glass phase during MB treatment.

Table 4. Reusability of ZCO_1 material (normal light, 60 minutes)

N°.	Catalyst recycle	Yield
1	Fresh	92.1
2	1st	89.5
3	2nd	85.3
4	3rd	79.6

The above results express the role of ZCO_1 material as a catalyst in the MB decomposition process. In this case, the ZCO_1 material does not act as an adsorbent, which is entirely in agreement with its small surface area.

In the experiments conducted above to study the catalytic ability of MB decomposition, air was freely diffused into the solution through the stirring process of the magnet bar. We hypothesized that the ZCO_1 catalyst containing K^+ holds oxygen and MB molecules simultaneously on the surface, promoting high-performance oxidation even under cold conditions.

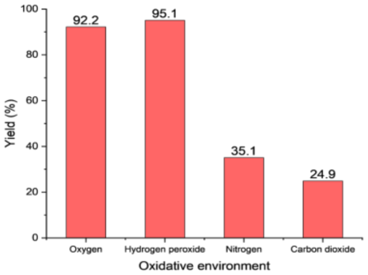

Figure 5. Effects of some substances on MB decomposition efficiency (60 minutes, normal light).

To clarify the oxidant source that decomposes MB, the processes were carried out in various oxidative environments, such as H_2O_2, N_2, and CO_2 (Figure 5).

Using different oxidative environments from two inert gas sources: nitrogen (very slightly soluble in water) and CO_2 (more soluble in water) was to control oxygen dissolved in the solution, reducing oxygen's influence on redox reactions on the catalyst surface. Besides, adding H_2O_2 is believed to provide another source of redox at the same time as dissolved oxygen or promote oxidation by the mechanism of the Fenton reaction.

Adding H_2O_2 (slightly) increases MB decomposition efficiency, while N_2 or CO_2 aeration significantly reduces it. However, there is no clear difference between the efficiencies of oxidation with the presence of only oxygen (92%) and the presence of oxygen and H_2O_2 (95%). Thus, the oxidant that decomposes MB may be oxygen in the air.

Table 5. Effect of initial K_2CO_3 amount on MB decomposition yield (60 minutes, darkness)

N°.	Molar rate of		Yield (%)
	K_2CO_3/ $Zn(NO_3)_2$	Zn:Co:K	
1	0	1:2:0	11.3
2	0.05	1:2:0.1	67.7
3	0.20	1:2:0.4	85.5
4	0.50	1:2:1	93.8
5	1.00	1:2:2	91.6

Table 5 shows that the presence of K^+ significantly increased MB decomposition efficiency. The best yield was achieved when the molar ratio Zn:Co:K = 1:2:1. The mechanism of K^+ ions promoting high-performance redox reactions without needing a heat or light source has yet to be specifically proven. However, the hypothesis can be considered that the presence of solid base K_2CO_3 makes the surface of ZCO more activated, reducing the amount of OH groups on the surface due to hydration by the aqueous solution, which also can directly affect the redox state of MB and the material itself. On the other hand, based on the EDX results, a part of K^+ may pervade into the ZCO crystal to create the holes or replace some metal cations Zn^{2+} or Co^{3+}, which increase the number of free electrons in the crystal lattice and can also be the cause of increased catalytic ability of the material.

4. Conclusion

Synthesized spinel nanomaterial $ZnCo_2O_4$ from nitrate salts of Zn^{2+} and Co^{2+} in the presence and absence of K_2CO_3 showed an optimistic result with the comprehensive studies of phase composition, chemical composition, and surface morphology of the material. As a result, the as-produced material has a crystalline phase of cubic spinel $ZnCo_2O_4$ with nanometer size. The composition of the material has a molar ratio of Zn:Co:K, similar to the original mixture of salts. The product has a relatively large size and small surface area. The presence of K_2CO_3 in the ZCO materials had significantly increased the catalytic ability of the material to decolor MB up to 95% in no need of heat or energy source of light, and the material had good reusability.

Reference

[1] M. Dhanasekar, S. Ratha, C. S. Rout, S. V. Bhat, Self-assembled Nanosheets of $ZnCo_2O_4$ as Efficient Sonophotocatalysts for Day Light Dye Degradation, Ceramics International, Vol. 48, No. 19, 2022, pp. 29460-29464, https://doi.org/10.1016/j.ceramint.2022.06.223.

[2] J. A. Rajesh, B. K. Min, J. H. Kim, H. Kim, K. S. Ahn, Cubic Spinel AB_2O_4 Type Porous $ZnCo_2O_4$ Microspheres: Facile Hydrothermal Synthesis and Their Electrochemical Performances in Pseudocapacitor, Journal Electrochemical Society, Vol. 163, No. 10, 2016, pp. A2418-A2427, https://doi.org/10.1149/2.0071613jes.

[3] Y. Gao, S. Cong, H. Yu, D. Zou, Investigation on Microwave Absorbing Properties of 3D C@$ZnCo_2O_4$ as a Highly Active Heterogenous Catalyst and the Degradation of Ciprofloxacin by Activated Persulfate Process, Separation Purification Technology, Vol. 262, No. November 2020, 2021, pp. 118330, https://doi.org/10.1016/j.seppur.2021.118330.

[4] J. Rashid, M. A. Barakat, R. M. Mohamed, I. A. Ibrahim, Enhancement of Photocatalytic Activity of Zinc/Cobalt Spinel Oxides by Doping with ZrO_2 for Visible Light Photocatalytic Degradation of 2-chlorophenol in Wastewater, Journal Photochemistry Photobiology: A Chemistry, Vol. 284, 2014, pp. 1-7, https://doi.org/10.1016/j.jphotochem.2014.03.017.

[5] B. Cui, H. Lin, X. C. Zhao, J. B. Li, W. Di Li, Visible Light Induced Photocatalytic Activity of $ZnCo_2O_4$ Nanoparticles, Wuli Huaxue Xuebao/ Acta Physico - Chimica Sinica, Vol. 27, No. 10, 2011, pp. 2411-2415, https://doi.org/10.3866/PKU.WHXB20110937.

[6] S. Hemamalini, R. Manimekalal, Synthesis, Physicochemical and Photocatalytic Activities of Nano $ZnCo_2O_4$ Catalyst for Photodegradation of Various Dyes under Sunlight Irradiation, Bulletin of Material Science, Vol. 44, No. 2, 2021, pp. 154-162, https://doi.org/10.1007/s12034-021-02453-y.

[7] V. Subhiksha, A. A. Alatar, M. K. Okala, I. A. Alaraidh, A. Mhebaldin, M. Aufy, M. A. A. Maksoud, L. L. Raju, A. M. Thomas, S. S. Khan, Double Z-Scheme $ZnCo_2O_4/MnO_2/FeS_2$ Photocatalyst with Enhanced Photodegradation of Organic Compound: Insights into Mechanisms, Kinetics, Pathway and Toxicity Studies, Chemosphere, Vol. 303, 2022, pp. 135177-135189, https://doi.org/10.1016/j.chemosphere.2022.135177.

[8] B. Tan, Y. Fang, Q. Chen, X. Ao, Y. Cao, Preparation of a $CaFe_2O_4/ZnCo_2O_4$ Composite Material and its Photocatalytic Degradation of Tetracycline, Optical Material, Vol. 109, 2020, pp. 110470-110484, https://doi.org/ 10.1016/j.optmat.2020.110470.

[9] W. Liu, S. Hu, Y. Wang, B. Zhang, R. Jin, L. Hu, Anchoring Plasmonic Ag@AgCl Nanocrystals onto $ZnCo_2O_4$ Microspheres with Enhanced Visible Photocatalytic Activity, Nanoscale Research Letters, Vol. 14, No. 1, 2019, pp. 108-123, https://doi.org/10.1186/s11671-019-2922-1.

[10] J. Yu, L. Lu, J. Li, P. Song, Biotemplated Hierarchical Porous-structure of ZnAl-LDH/$ZnCo_2O_4$ Composites with Enhanced Adsorption and Photocatalytic Performance, RSC Advances, Vol. 6, No. 16, 2016, pp. 12797-12808, https://doi.org/10.1039/C5RA15758G.

[11] J. M. Gonçalves, M. I. Silva, M. N.T. Silva, P. R. Martins, E. Nossol, H. E. Toma, L. Angnes, Recent Progress in $ZnCo_2O_4$ and its Composites for Energy Storage and Conversion: A Review, Energy Advances, No. 11, 2022, pp. 793-841, https://doi.org/10.1039/d2ya00106c.

[12] N. S. Bajaj, R. A. Joshi, Energy Materials: Synthesis and Characterization Techniques, in Energy Materials, Elsevier, 2021, pp. 61-82, https://doi.org/10.1016/B978-0-12-823710-6.00019-4.

[13] V. T. Tan, L. T. Vinh, T. N. Khiem, H. D. Chinh, Facile Template In-situ Fabrication of $ZnCo_2O_4$ Nanoparticles with Highly Photocatalytic Activities under Visible-light Irradiation, Bulletin of Chemical Reaction Engineering and Catalysis, Vol. 14, No. 2, 2019, pp. 404-412, https://doi.org/10.9767/bcrec.14.2.3613.404-412.

[14] Z. Jiang, L. Feng, J. Zhu, X. Li, S. Khan, Y. Chen, Enhanced Visible-light Utilization with $ZnCo_2O_4$–$BiErWO_6$ Heterojunctions Towards Photocatalytic Degradation of Antibiotics, Journal Material Science: Materials in Electronics, Vol. 31, No. 20, 2020, pp. 18248-18262, https://doi.org/10.1007/s10854-020-04373.